Study of the Perpendicular Band Intensities of the CH Chromophore in $CHCl_3$, $CHBr_3$, and CHI_3 with Three-Dimensional Dipole Moment Surface from Density Functional Calculations

Sheng-Gui He,* Lan-Feng Yuan, Hai Lin,† and Qing-Shi Zhu

Open Laboratory of Bond Selective Chemistry, and the Institute for Advanced Studies, University of Science and Technology of China, Hefei, 230026, P. R. China

Xiao-Gang Wang

Departement de chimie, Universite de Montreal, C.P. 6128, succursale Centre-ville, Montreal, Quebec H3C 3J7, Canada

Received: November 7, 2000; In Final Form: June 27, 2001

The fundamental and overtone absolute intensities of the perpendicular band of the isolated CH chromophore in chloroform ($CHCl_3$), bromoform ($CHBr_3$), and iodoform (CHI_3) have been calculated. The calculations were carried out by employing a three-dimensional curvilinear internal coordinate Hamiltonian and a polynomial expanded three-dimensional dipole moment surface (DMS). The DMS was obtained by a hybrid density functional method. Molecular symmetry was used to deduce the appropriate DMS expansion formulas. The calculated band intensities were compared with available experimental data. Most predicted values are accurate to within a factor of 2.

I. Introduction

The intensities of fundamental and overtone spectra of the CH chromophore in trihalomethanes (CHX_3, X = F, Cl, Br, and I) have drawn much attention. The primary motivation lies in two aspects. First, the transition intensities, in addition to the frequencies, are essential pieces of spectroscopic information for identifying the intramolecular mode−mode couplings in a quantitative manner. Trihalomethanes are chosen for the study because they are simple and good examples for investigating such couplings. Actually, it has been found, especially by Quack's group,[1] that the CH stretching and bending vibrations which are strongly coupled by Fermi resonance[2] can be dynamically isolated from the CX_3 frame. This behavior is related to a rapid intramolecular vibrational energy redistribution between the CH stretching and bending modes but a slow energy flow from the CH chromophore to the CX_3 frame.[1,3] Second, the molecular dipole moment surface (DMS) involved in the infrared intensity is usually difficult to obtain directly from the experiment. An alternative way is to compute with the ab initio or density functional theory (DFT) method. The infrared absorption intensities can be used to verify the validity of such calculated DMS and, consequently, to test the accuracy of these methods.

There are many experimental studies on the vibrational band intensities for CHF_3,[4−8] $CHCl_3$,[8−10] $CHBr_3$,[11−13] and CHI_3.[14] The measurements were mainly carried out with a Fourier transform spectrometer in the infrared region[4,8,12,14] and a photoacoustic spectrometer[8,10,13] in the visible region. The absolute band intensities of these trihalomethanes have been reported except for CHI_3. For CHF_3[4,8] and $CHCl_3$,[8,9] the intensity uncertainties were claimed to be less than 20−30% for most of the bands. As for $CHBr_3$, the uncertainties were not given. It should be pointed out that two definitions of intensity, the integrated "strength" (G) and the integrated "intensity" (I), have been frequently used in the experimental reports:

$$G = \int \sigma(\nu)\, \mathrm{d}(\ln\nu) \tag{1}$$

$$I = \int \sigma(\nu)\, \mathrm{d}\nu \tag{2}$$

where σ is the absorption cross section at wavenumber ν. Approximately, the relationship between these two definitions is as follows:

$$I = G\nu_0 \tag{3}$$

where ν_0 denotes the band origin of the transition. In this work, the definition of integrated intensity (I) is adopted.

Theoretical investigations on the vibrational band intensities of CH chromophore can be mainly divided into two types which differ in the ways of obtaining the DMS. The first type[9,15−20] uses the parameter adjustable empirical dipole moment function to calculate the intensities. The Mecke-type function[21] is widely used because it has the correct asymptotic behavior as the bond length approaches infinity and contains only three parameters. This type of study assumes that the CH stretching vibration carries all the intensity and the bending or stretching-bending combination bands borrow intensity from the pure stretching via wave function mixing. This method helps to understand the strong Fermi resonance between the CH stretching and bending, especially in the high overtone regions. The drawbacks of this method are that (1) the DMS should be determined by the observed intensities so that it cannot predict the intensities if no experimental data are available and (2) some band intensities of the bending or stretching−bending combinations in the low-

* Author to whom correspondence should be addressed. Email: hsg@mail.ustc.edu.cn.

† Current address: Anorganische Chemie, Fachbereich9, Universität-Gesamthochschule Wuppertal, D-42097 Wuppertal, Germany.

10.1021/jp0040906 CCC: $20.00
Published on Web 08/17/2001

TABLE 1: Grid Arrangements in the DFT Calculations of the Dipole Moment Surface for CHX_3 (X = Cl, Br, and I)[a]

	$CHCl_3$			$CHBr_3$			CHI_3		
	from	to	step	from	to	step	from	to	step
r (Å)[b]	−0.4	0.8	0.1	−0.4	0.4	0.1	−0.4	0.4	0.1
ϕ_1 (deg)	−20	15	5	−16	16	*d*	−16	16	*d*
ϕ_2 (deg)	−20	20	5[c]	−16	16	*d*	−16	16	*d*
no. of points		433			405			405	

[a] See text for the definitions of r, ϕ_1, and ϕ_2. Constrain $\phi_1 \leq \phi_2$ in the DFT calculations. [b] 1 Å = 10^{-10} m. [c] The steps are set to 10° at $\phi_1 = -20°$ and −10° when $r \leq 0.4$ Å. [d] The steps for ϕ_i (i = 1 and 2) are −16°, −8°, −4°, −2°, 0°, 2°, 4°, 8°, and 16°.

energy region cannot be well reproduced due to the neglect of the cross terms in the multidimensional DMS.[22]

Another way to obtain the DMS is to use the ab initio or DFT calculations. Both parallel and perpendicular bands of CHF_3 were investigated by Quack's group[17,23,24] using the DMS from the configuration interaction with single and double excitation (CISD) method. The parallel band intensities of $CHCl_3$,[22] $CHBr_3$,[25] and CHI_3[26] were studied in our earlier works using the DMS from the DFT calculations. The predictions were found to be quite successful. Moreover, the anomalous strong first stretching overtone of $CHCl_3$ is found to be mainly due to the strong nonlinearity of the DMS near equilibrium configuration.

The success of our earlier investigations on the parallel band intensities of $CHCl_3$, $CHBr_3$, and CHI_3 based on the DFT DMS stimulated us to analyze the perpendicular band, which is the main purpose of this work. The outline of the remainder of this article is as follows. In section II, we report on the three-dimensional (3D) DMS obtained from the DFT calculations. The x and y components of the dipole moment vector along the molecule-fixed axes are evaluated. Molecular symmetry is used to derive the DMS expansion function in terms of curvilinear internal coordinates.[18,27] In section III, the absolute band intensities are calculated. The results are compared with the experimental data and discussed in section IV, and a summary is made in section V.

II. Dipole Moment Surface

The computational method for the 3D DMS of $CHCl_3$, $CHBr_3$, and CHI_3 has been detailed in our earlier works.[22,25,26] Briefly, the B3PW91[28] hybrid density functional with the basis sets of LanL2DZ[29] for I atom and 6-311++G(3df,2pd)[30] for the other atoms have been adopted in the calculations. The following notations are employed: r is the CH bond length displacement, and ϕ_i (i = 1, 2, and 3) is the displacement of the angle H−C−X_i, where X_i is the ith X atom in the CX_3 frame. When evaluating the dipole moment, only the CH bond is stretched or bent, while the remaining CX_3 frame is kept at its equilibrium configuration. Here, we summarize the grid arrangements in the DFT calculations in Table 1. The dipole moment vector **M** has three components M_x, M_y, and M_z, with x, y, and z being the principal inertial axes of the CX_3 frame which is held to its equilibrium. M_z which leads to the parallel transition[31] has been studied in our earlier works;[22,25,26] here, we shall describe M_x and M_y, which are associated with the perpendicular transition.

In the earlier investigations,[22,25,26] the polynomial functions in terms of curvilinear internal coordinates[18,27] were successfully used to represent M_z and to calculate the parallel band intensities. They are adopted here as well for M_x and M_y. The CH stretching coordinate is defined as

$$r = R - R_e \tag{4}$$

where R is the instantaneous CH bond length and R_e the equilibrium value taken from the DFT optimization. The CH bending coordinates are defined as

$$\theta_1 = (2\phi_1 - \phi_2 - \phi_3)/\sqrt{6} \tag{5}$$

$$\theta_2 = (\phi_2 - \phi_3)/\sqrt{2} \tag{6}$$

In this work, the X atoms in CX_3 frame are labeled such that θ_1 and θ_2 defined in the above equations have the same symmetry as M_x (E_a) and M_y (E_b), respectively. Here E_a and E_b denote the two components of the E representation of the C_{3v} point group. So M_x and M_y can be expanded as follows:

$$M_x(r,\theta_1,\theta_2) = \sum_m \sum_{p-q=3n\pm1} C^x_{mpq} r^m (\theta^p_+ \theta^q_- + \theta^q_+ \theta^p_-)/2 \tag{7}$$

$$M_y(r,\theta_1,\theta_2) = \sum_m \sum_{p-q=3n\pm1} C^y_{mpq} r^m (\theta^p_+ \theta^q_- - \theta^q_+ \theta^p_-)/2i \tag{8}$$

where C^x_{mpq} and C^y_{mpq} are expansion coefficients, m, n, p, and q are nonnegative integers, $p - q \geq 0$, and $\theta_\pm = \theta_1 \pm i\theta_2$. In this work, we only include terms with (p, q) = (1, 0), (2, 0), and (2, 1). The reason will be discussed at the end of this section. If C^1_3 is one of the C_3 rotations in the C_{3v} point group, we have[32]

$$C^1_3(M_x + iM_y) = \exp(i2\pi/3)(M_x + iM_y) \tag{9}$$

$$C^1_3(\theta_\pm) = \exp(\pm i2\pi/3)\theta_\pm \tag{10}$$

Applying the above two equations, it is straightforward to find the following simple relations:

$$C^x_{mpq} = C^y_{mpq}, \text{ when } p - q = 3n + 1 \tag{11}$$

$$C^x_{mpq} = -C^y_{mpq}, \text{ when } p - q = 3n - 1 \tag{12}$$

The expansion coefficients are obtained by fitting to the symmetry unique DFT data points in Table 1. In the practical fitting of the DMS, it is, however, not necessary to include many high-order terms. For example, those terms ($p - q > 3$ in eqs 7 and 8) related to the coupling of the states with large difference in the vibrational angular momentum quantum number are negligible because there is so far no experimental evidence supporting this kind of coupling.[24] Moreover, the accuracy of the DFT calculations may not be sufficient to determine them. The fitted expansion coefficients of M_x and M_y are collected in Table 2. Some data points in Table 1 are not used in the fitting due to relatively large fitting errors. For $CHCl_3$, the data points of $r \geq 0.6$ Å and $\theta \geq 35°$ are discarded, where $\theta = \sqrt{\theta_1^2+\theta_2^2}$. For $CHBr_3$ and CHI_3, those of $\theta \geq 30°$ are not used. The numbers of the symmetry unique data points used in the fitting are 261, 378, and 378 for $CHCl_3$, $CHBr_3$, and CHI_3, respectively.

III. Intensity Calculations

The absolute vibrational band intensity I can be calculated as

$$I = \frac{1}{4\pi\epsilon_0}\frac{8\pi^3\nu_0}{3hcQ_v(T)}\left[1 - \exp\left(-\frac{hc\nu_0}{kT}\right)\right]|\langle f|\mathbf{M}|i\rangle|^2 \tag{13}$$

TABLE 2: Expansion Coefficients[a] of the *x* and *y* Components of the Dipole Moment Surface for CHX_3 (X = Cl, Br, and I) Obtained by Fitting to the DFT Calculated Data Points[b]

coeffs	$CHCl_3$	$CHBr_3$	CHI_3
$C^x_{010} = C^y_{010}$	0.24828(65)	0.43131(37)	0.72214(58)
$C^x_{020} = -C^y_{020}$	0.16059(84)	0.17169(56)	0.19744(89)
$C^x_{021} = C^y_{021}$	−0.2488(29)	−0.3188(21)	−0.3682(34)
$C^x_{110} = C^y_{110}$	−0.5811(27)	−0.5859(18)	−0.6312(29)
$C^x_{121} = C^y_{121}$	−0.2552(89)	−0.4721(82)	−0.726(13)
$C^x_{210} = C^y_{210}$	0.6007(38)	0.5480(24)	0.5431(38)
$C^x_{220} = -C^y_{220}$	−0.3908(64)	−0.4257(63)	−0.394(10)
$C^x_{310} = C^y_{310}$	0.467(13)	0.690(11)	0.897(18)
rms[c]	2.37×10^{-3}	1.28×10^{-3}	2.03×10^{-3}

[a] Units are defined such that the dipole moment is in Debye (= 3.33564×10^{-30} C m), the bond length and the bond angle displacements in Å (= 10^{-10} m) and radian, respectively. [b] The values given in the parentheses are 1 standard error in the last significant digit. See text for details. [c] Root-mean-squares of the fitting residual in Debye.

where ν_0 is the transition wavenumber from the initial state $|i\rangle$ to the final state $|f\rangle$ in cm^{-1}, **M** is the dipole moment function, T is the sample temperature in the measurement, $Q_v(T)$ is the vibrational partition function at temperature T, c is the speed of light, ϵ_0 is the permittivity of vacuum, and k and h are Boltzmann and Planck constants, respectively. It should be pointed out that for the CH chromophore vibrational transition in $CHCl_3$, $CHBr_3$, and CHI_3, the hot bands associated with the low-frequency frame vibrations are strong if the measurement is carried out at room temperature or higher. However, this kind of hot bands is almost superposed with the corresponding cold bands because the coupling between the CH chromophore and the frame vibrations is weak. At least the experiment with medium or low resolution cannot resolve them successfully; thus, the experimental intensity will include contributions from the hot bands, which is the case for the experimental reports of these three molecules under study.

Therefore, to study the CH chromophore band intensities, eq 13 should become

$$I_{N_j} = \frac{1}{4\pi\epsilon_0}\frac{8\pi^3\nu_0}{3hcQ_v(T)}\left[1 - \exp\left(-\frac{hc\nu_0}{kT}\right)\right]\sum_n \exp\left(-\frac{E_n}{kT}\right)|\langle N_j,n|\mathbf{M}|0_1,n\rangle|^2 \quad (14)$$

where n and N_j denote the vibrational quantum numbers for the frame and the chromophore, respectively, and E_n is the vibrational energy of $|0_1,n\rangle$ state. Here the notation N_j used by Dübal and Quack[3] is adopted. $N = \upsilon_s + \upsilon_b/2$, where υ_s and υ_b are the CH stretching and bending vibrational quantum numbers, respectively, and j is the counting index from highest to lowest states within a multiplet. In this work, the following approximations are made to calculated the intensity in eq 14. (1) The frame and the chromophore motions are assumed to be dynamically isolated, i.e., $|N_j,n\rangle = |N_j\rangle|n\rangle$. (2) The expectation value $\mathbf{M}_n = \langle n|\mathbf{M}|n\rangle$ is replaced by the 3D CH chromophore DMS described in the previous section because the dependence of **M** upon the frame coordinates is not explicitly calculated. The error of the above two approximations is on the order of the difference between the calculated and the experimental value of the dipole moment[23] and shall be discussed later. (3) $\exp(-hc\nu_0/kT) \simeq 0$, and the reduced vibrational partition function in the chromophore subspace $Q_v(T)/\sum_n \exp(-E_n/kT) \simeq 1$. This approximation overestimates the calculated intensities by about 1%, 1%, and 8% for the bending fundamentals of $CHCl_3$ (1120 cm^{-1}), $CHBr_3$ (1148 cm^{-1}), and CHI_3 (1070 cm^{-1}), respectively, and about two-thirds of the corresponding values for the other bands. Here, T = 296, 296, and 433 K are respectively used in the estimation for $CHCl_3$, $CHBr_3$, and CHI_3 considering the experimental conditions.[8,9,12−14] From the dipole transition selection rule for the molecules with C_{3v} symmetry[31] and applying the above approximations to eq 14, the perpendicular band intensity $I_\perp$ is given as

$$I_\perp = K\nu_0(|\langle N_j|M_x|0_1\rangle|^2 + |\langle N_j|M_y|0_1\rangle|^2) \quad (15)$$

where $K = 4.1623755 \times 10^{-19}$ cm^2 D^{-2} (1 D = 3.33564×10^{-30} C m).

A reduced 3D Hamiltonian model in terms of the curvilinear internal coordinates in ref 20 is used to calculate the wave functions and transition wavenumbers. The details about the Hamiltonian and the variational calculations of the wave functions can be found in that reference and are omitted here. The basis used in the variational calculations is the product of Morse function for the stretch and two-dimensional isotropic harmonic oscillator function for the bend. The necessary matrix elements of the DMS operators in above basis can be found in refs 18, 25, and 32 or easily derived from the basic formulas listed in them. The potential energy parameters of $CHCl_3$ and $CHBr_3$ are taken from ref 20, and those of CHI_3 are taken from the last column of Table 2 of ref 26. The absolute intensities of the perpendicular band are then calculated using the DMS obtained in the previous section. For comparison, the absolute parallel band intensities are also calculated by use of the two-dimensional z component DMS for $CHCl_3$,[22] $CHBr_3$,[25] and CHI_3[26] in the earlier works. After the absolute intensities are calculated, the intrapolyad relative intensities are calculated as I_{N_j}/I_N and $I_N = \sum_j I_{N_j}$, which is defined as the interpolyad intensity.

IV. Results and Discussion

The calculated and observed absolute band intensities are given for $CHCl_3$ and $CHBr_3$ in Tables 3 and 4, respectively. In the case of CHI_3, no observed absolute intensities have been reported in the literature. Fortunately, the nice illustration of the spectra of CHI_3in ref 14 enables us to estimate the intensities for some strong transitions. A brief description of the estimation is given as follows. The absorbance profile of the $N_j = 3_1$ band in Figure 6 of ref 14 is simulated by a triangle with the bottom side length 17 cm^{-1} and height 0.24. The integral of the absorbance for this band is $\ln(10) \times 17 \times 0.24/2 = 4.70$ cm^{-1}. Considering the experimental conditions for this spectrum, the absolute intensity for 3_1 band is 110×10^{-22} cm. Similar procedure gives the values of 3900×10^{-22} cm and 1100×10^{-22} cm for the Q branches of 1_1 band in Figure 3 and 2_1 band in Figure 5 in ref 14, respectively. The overall band intensity in this case is estimated to be 3 times the value of the Q branch. Comparing the $(^5/_2)_1$ band with 3_1 band in Figure 1c and assuming the intensity is proportional to the peak height, the value of $110 \times 10^{-22} \times 0.4/0.24 = 180 \times 10^{-22}$ cm is obtained for the intensity of $(^5/_2)_1$ band. Similarly, $(^3/_2)_1$ band intensity is estimated in Figure 1a by comparing with the 1_1 band, which gives the value of $3 \times 3900 \times 10^{-22}/2.5 = 4700 \times 10^{-22}$ cm. Table 5 gives the estimated and calculated intensities for CHI_3. For illustration, the observed and calculated interpolyad intensities of $CHCl_3$ and $CHBr_3$ are plotted in Figure 1.

It can be seen that in this work, the E symmetry 3D dipole moment components M_x and M_y are successfully described by

TABLE 3: Observed and Calculated Vibrational Transition Wavenumbers (in cm^{-1}) and Absolute Intensities (in 10^{-22} cm) of $CHCl_3$[a] (the Intrapolyad Relative Intensities Are Also Listed)

	observation			calculation		
N_j	ν_0	I^{Abs}	I^{Rel} [b]	ν_0	I^{Abs}	I^{Rel} [b]
$(1/2)_1$	1219.8	...	...	1221.5	9050.4	1
1_2	2410[c]	321	0.55	2414.0	1295.8	0.45
1_1	3033[c]	262	0.45	3034.6	1575.5	0.55
$(3/2)_2$	3598	...	...	3602.3	2.65	0.0015
$(3/2)_1$	4234.9	1700	...	4237.3	1743.4	1.00
2_3	4762	17	0.0054	4760.8	16.4	0.0039
2_2	5401	200	0.064	5408.8	224.5	0.053
2_1	5941	2930	0.93	5942.7	3973.4	0.94
$(5/2)_3$	...	...	...	5914.6	0.051	0.000 25
$(5/2)_2$	6569	9.0	0.045	6575.8	8.74	0.043
$(5/2)_1$	7129	190	0.95	7127.8	193.6	0.96
3_4	...	...	...	7038.1	0.022	0.0001
3_3	...	...	...	7711.1	0.67	0.0030
3_2	8278	11	0.087	8278.1	10.2	0.046
3_1	8727	115	0.91	8725.1	211.0	0.95
$(7/2)_3$	...	...	...	8841.5	0.026	0.0018
$(7/2)_2$	9425	4.7	0.14	9423.8	1.46	0.10
$(7/2)_1$	9899	28	0.86	9894.1	13.0	0.90
4_4	...	...	...	9939.8	0.003	0.000 25
4_3	...	...	...	10535.1	0.037	0.0027
4_2	11 019	0.4	0.077	11022.5	0.78	0.056
4_1	11 385	4.8	0.92	11383.4	13.05	0.94
$(9/2)_3$	...	...	...	11641.5	0.011	0.0093
$(9/2)_2$	12 151	...	...	12146.7	0.24	0.19
$(9/2)_1$	12 552	...	...	12539.0	1.00	0.80
5_3	...	...	...	13232.8	0.0024	0.0022
5_2	13 635	0.045	0.16	13642.7	0.106	0.096
5_1	13 921	0.23	0.84	13921.4	0.996	0.90
$(11/2)_3$	14 312	0.003		14314.4	0.0043	0.032
$(11/2)_2$	...	...	...	14744.9	0.042	0.32
$(11/2)_1$	...	...	...	15067.7	0.086	0.65
6_2	16 132	0.0092	0.33	16136.8	0.025	0.22
6_1	16 349	0.019	0.67	16349.3	0.085	0.77
$(13/2)_2$	...	...	...	17490.5	0.0073	0.43
$(13/2)_1$	...	...	...	17217.5	0.0083	0.49
7_2	...	...	...	18496.6	0.007	0.53
7_1	...	...	...	18691.9	0.006	0.45
Δ[d]					0.772[e]	0.276

[a] Transitions of which the calculated intensities greater than 2.0×10^{-25} cm are listed. Experimental data are taken from refs 8, 9, and 44. N and j are the notations used by Dübal and Quack;[4] see text. [b] Intrapolyad relative intensity. [c] Overlapped by other bands. [d] Logarithmic deviation; see text. [e] $N = 1$ polyad excluded, else $\Delta = 0.880$. $\Delta = 0.569$ if $N = 1$, 5, 11/2, or 6 polyad excluded.

TABLE 4: Observed and Calculated Vibrational Transition Wavenumbers (in cm^{-1}) and Absolute Intensities (in 10^{-22} cm) of $CHBr_3$[a] (the Intrapolyad Relative Intensities Are Also Listed)

	observation			calculation		
N_j	ν_0	I^{Abs}	I^{Rel} [b]	ν_0	I^{Abs}	I^{Rel} [b]
$(1/2)_1$	1148.1	83 811	1	1151.0	29264.2	1
1_2	2269.5	1702	0.24	2275.0	3138.8	0.29
1_1	3048.1	5334	0.76	3050.1	7784.8	0.71
$(3/2)_2$	3392.4	17	0.0081	3395.5	33.8	0.013
$(3/2)_1$	4181.5	2070	0.99	4182.1	2488.4	0.99
2_3	4488.5	0.86	0.0003	4488.3	0.862	0.000 26
2_2	5284.7	152	0.053	5285.8	145.2	0.043
2_1	5969.6	2694	0.95	5972.5	3204.5	0.96
$(5/2)_3$	...	...	...	5577.0	0.049	0.0002
$(5/2)_2$	6389.6	7.7	0.055	6385.6	7.80	0.032
$(5/2)_1$	7084.1	133	0.94	7086.0	235.4	0.97
3_2	8181.0	4.1	0.047	8169.4	2.26	0.017
3_1	8766.0	82.3	0.95	8767.4	127.86	0.98
$(7/2)_3$	...	...	...	8523.1	0.013	0.000 94
$(7/2)_2$	...	...	...	9248.7	1.12	0.077
$(7/2)_1$	9867.0	5.9	...	9863.2	13.35	0.92
4_3	...	...	...	10297.4	0.0066	0.0011
4_2	...	...	...	10926.2	0.022	0.0036
4_1	11429.9	3.4	...	11435.5	6.09	1.00
$(9/2)_3$	...	...	...	11341.6	0.0054	0.0051
$(9/2)_2$	11998.2	...	0.22	11985.0	0.14	0.14
$(9/2)_1$	12509.1	...	0.78	12514.7	0.89	0.86
5_3	...	...	...	13011.0	0.0041	0.011
5_2	13548.0	0.0049[c]	0.019	13557.1	0.000 22	0.0006
5_1	13975.3	0.25[c]	0.98	13977.6	0.36	0.99
$(11/2)_2$	14582.2	...	0.074	14595.2	0.021	0.22
$(11/2)_1$	15046.0	...	0.93	15042.1	0.070	0.76
6_3	...	...	...	15597.5	0.0015	0.053
6_2	16061.0	0.001	0.077	16063.2	0.000 29	0.010
6_1	16403.2	0.012	0.92	16396.0	0.027	0.93
$(13/2)_2$	...	...	...	17080.1	0.0032	0.32
$(13/2)_1$	...	...	...	17448.8	0.0063	0.63
7_1	...	...	...	18695.9	0.0026	0.79
Δ[d]					0.612[e]	0.440[f]

[a] All available experiment detected transitions are listed, and the transitions of which the calculated intensities greater than 1.5×10^{-25} cm are also listed; experimental data are taken from refs 12 and 13. N and j are the notations used by Dübal and Quack;[4] see text. [b] Intrapolyad relative intensity. [c] HD standard used in the photoacoustic experiments (see ref 12). Ethane standard experiment gives: $I(5_2) = 0.24 \times 10^{-24}$ cm, $I(5_1) = 0.12 \times 10^{-22}$ cm. [d] Logarithmic deviation; see text. [e] $N_j = 5_2$ band excluded, else $\Delta = 0.943$. $\Delta = 0.475$ if $N = 1/2$, 5, or 6 polyad excluded. [f] $N = 5$ and 6 polyads excluded, else $\Delta = 0.980$.

the same number (eight) of independent expansion coefficients as those used in the earlier work[22] for M_z with A_1 symmetry. In Tables 3−5, the agreement between the calculation and the observation is within a factor of 2 for most of the bands. The agreement for perpendicular bands (N = half odd number) is slightly better than that for parallel bands (N = integer). We note that the agreement is quite good for CHI_3 of which the experimental absolute intensities are roughly estimated. Logarithmic deviation[23] defined as

$$\Delta = \left\{ \frac{1}{n_{dat}} \sum_{i=1}^{n_{dat}} [\ln(I_i^{calc}/I_i^{obs})]^2 \right\}^{1/2} \qquad (16)$$

is applied to show the overall agreement between the calculation and the observation. Here n_{dat} is the number of the experimental data points. The deviations for the absolute intensities are 0.772 for $CHCl_3$, 0.612 for $CHBr_3$, and 0.313 for CHI_3. The deviations for the intrapolyad relative intensities are 0.276, 0.440, and 0.586 for $CHCl_3$, $CHBr_3$, and CHI_3, respectively.

It should be pointed out that large discrepancies between the calculation and the observation exist for a few parallel bands, such as 1_2 and 1_1 bands of $CHCl_3$, 5_2 and 6_2 bands of $CHBr_3$, and 3_2 band of CHI_3. The explanations which have been given or discussed in the earlier works[22,25,26] are omitted here since this work focuses on the perpendicular bands. Except for the above-mentioned bands, the overall deviation is still larger than the experimental uncertainty, which, for instance, is stated as less than about 20% for $CHCl_3$.[9] Two factors, the vibrational wave functions and the dipole moment functions, can lead to errors in the intensity calculations. In this work, the Hamiltonian model described in the CH chromophore subspace by use of the curvilinear internal coordinates is adopted to calculate the wave functions. This incomplete description of the full vibrational problem will lead to calculation errors. It has been argued that there are two dominant mechanisms for such intensity effects: the "geometrical" contribution from the movement of the large CX bond dipole and the change of the charge distribution in the highly polarizable CX_3 frame. It is likely that the Hamiltonian model in terms of polar normal coordinates[32] will present better intensity results because in this model, harmonic coupling between the CH chromophore and the CX_3 frame vibrations is considered but not in the curvilinear internal coordinate model.[1,17,23]

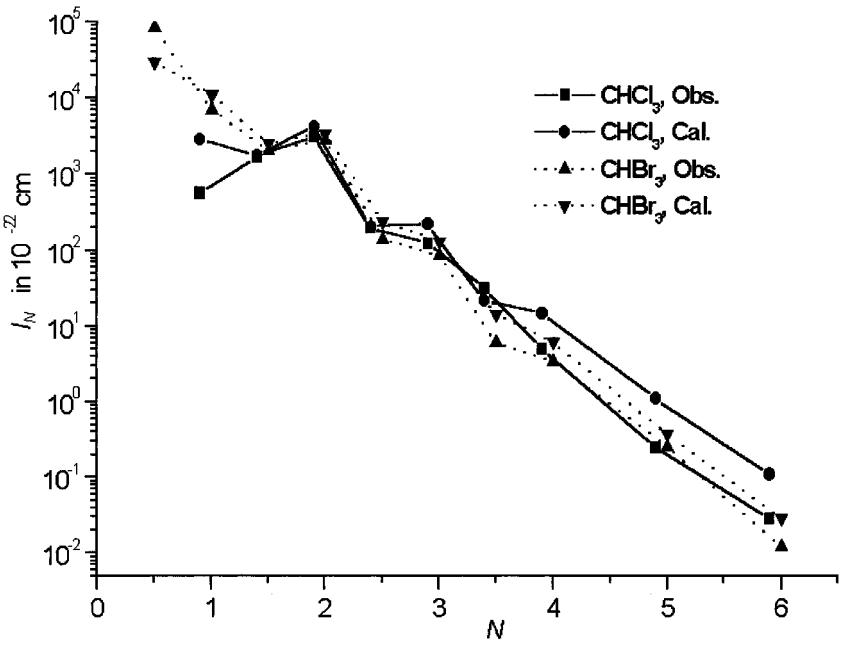

Figure 1. Observed and calculated interpolyad intensities of $CHCl_3$ and $CHBr_3$.

TABLE 5: Observed and Calculated Vibrational Transition Wavenumbers (in cm^{-1}) and Absolute Intensities (in 10^{-22} cm) of CHI_3[a] (the Intrapolyad Relative Intensities Are also Listed)

	observation			calculation		
N_j	ν_0	I^{Abs}	$I^{Rel\ b}$	ν_0	I^{Abs}	$I^{Rel\ b}$
$(1/2)_1$	1070.0	...	...	1069.8	87062.1	1
1_2	2117.18	...	0.16	2117.1	926.2	0.087
1_1	3031.76	12 000	0.84	3031.6	9761.5	0.91
$(3/2)_2$	3165.0	...	...	3164.1	150.0	0.034
$(3/2)_1$	4086.5	4700	...	4085.9	4220.4	0.96
2_3	...	...	...	4188.2	23.6	0.0069
2_2	5117.80	...	0.035	5116.8	38.5	0.011
2_1	5937.25	3300	0.96	5937.4	3363.5	0.98
$(5/2)_3$	...	...	...	5211.8	0.26	0.000 72
$(5/2)_2$	6148.0	...	...	6147.3	11.7	0.033
$(5/2)_1$	6977.0	180	...	6976.7	343.4	0.97
3_4	...	...	...	6212.1	0.034	0.000 27
3_3	...	...	...	7154.0	0.68	0.0054
3_2	7992	...	0.018	7991.3	0.14	0.0011
3_1	8718.5	110	0.98	8717.9	126.0	0.99
$(7/2)_3$	...	...	...	8160.0	0.025	0.0013
$(7/2)_2$	...	...	...	9005.3	1.9	0.10
$(7/2)_1$	9743.0	...	...	9742.5	16.9	0.89
4_3	...	...	...	9994.4	0.020	0.0035
4_2	...	...	...	10740.8	0.022	0.0040
4_1	...	...	...	11373.1	5.6	0.99
$(9/2)_3$	...	...	...	10982.7	0.010	0.0083
$(9/2)_2$	...	...	...	11738.4	0.23	0.19
$(9/2)_1$	...	...	...	12383.9	0.98	0.80
5_2	...	...	...	13366.0	0.013	0.042
5_1	...	...	...	13903.7	0.30	0.96
$(11/2)_2$	...	...	...	14347.2	0.029	0.29
$(11/2)_1$	...	...	...	14901.9	0.067	0.68
6_1	...	...	...	16310.7	0.020	0.83
Δ[c]					0.313	0.586[d]

[a] Transitions of which the calculated intensities greater than 1.0×10^{-24} cm are listed. Observed transition wavenumbers and intrapolyad intensities are taken from ref 14. The observed absolute intensities are estimated in this work from the spectra in ref 14; see text for details of the estimation. N and j are the notations used by Dübal and Quack;[4] see text. [b] Intrapolyad relative intensity. [c] Logarithmic deviation; see text. [d] $N = 3$ polyad excluded, else $\Delta = 1.26$

However, Table 3 shows that for the absolute intensity of $CHCl_3$, the discrepancy between the calculation and the observation in the low overtone region ($N = {}^3/_2$, 2, and ${}^5/_2$) is within the stated experimental uncertainty (except for the 2_1 band). The discrepancy becomes large as the polyad number N increases. The investigations in refs 9, 23, 25, 34, and 35 have shown that the calculated band intensity is more sensitive to the DMS than to the potential energy surface. Moreover, as discussed earlier, the DFT calculations may not be accurate enough to determine the high-order terms in the DMS expansion, which have significant contributions to the intensities of the bands with high quantum numbers being excited.[22,36] Therefore, the errors from the DMS are most probably of the primary importance for the problem in question.

As shown in ref 37, to get the result with the best separation of vibrational and rotational motion, the reference frame which obeys Eckart conditions[38,39] should be used when evaluating the dipole moment components. Test calculation indicates that the maximal Euler angles[39] (in deg) between the Eckart axes[39] and the axes adopted in this work are only 0.711, 0.238, and 0.116, occurring at the configurations of (r/Å, ϕ_1/deg, ϕ_2/deg) = (0.8, 10, 20), (0.4, 16, 16), and (0.4, 16, 16) for $CH^{35}Cl_3$, $CH^{79}Br_3$, and $CH^{127}I_3$, respectively. It is shown that the frame used in this work is a good approximation to the Eckart frame. Similar results have been demonstrated for PH_3 in ref 40. Thus, the induced error due to the neglect of the Eckart conditions is negligible in this work. One may argue that the polynomials used in the dipole moment model do not have correct asymptotic behavior for molecular DMS, which will lead to calculation errors. The boundary conditions of the DMS will be important for the highly excited overtones. However, it is less critical for the low and medium energy regions ($N \leq 6$) studied in this work. In these regions, a good fit of the DMS near the equilibrium configuration has been demonstrated to be more important.[25,34,41] In this work and the earlier works,[22,25,26] the polynomial expansions can represent the DFT data points in a wide range of the vibrational coordinates within the accuracy of about 10^{-3} and 10^{-2} D for the E and A_1 symmetry DMS components, respectively. Thus, the errors coming from the polynomial dipole moment model are believed not to be important.

In conclusion, we believed that the errors from the DFT calculations are most important to account for the relatively large disagreement between the calculated and the observed intensities. This is further corroborated by the intensity investigations of SiH chromophore in $SiHD_3$[42] and $SiHF_3$,[36] where the higher-level CCSD(T)[43] coupled cluster method gives more accurate results than the DFT method. However, such high-level computation is expensive, especially in the cases of multidimensional DMS and polyatomic molecules with many electrons. Therefore, the DFT method with the basis sets employed in this work is a good compromise between the accuracy and computational cost.

V. Summary

The DFT method has been applied to calculate the 3D DMS of the CH chromophore of $CHCl_3$, $CHBr_3$, and CHI_3. The two *E* symmetry dipole moment components have been modeled by the polynomial expansion in terms of the curvilinear internal coordinates with limited number of independent coefficients and have been used to predict the absolute perpendicular band intensities of the CH chromophore. The calculations agree with the experimental data within a factor of 2 for most of the observed bands. The discrepancies between the calculation and the observation are discussed and found most probably to arise from the DFT calculations. The method developed in this work and our earlier works (for parallel bands) will be useful to test the validity of the DMS calculated by other ab initio or DFT methods for these molecules.

Acknowledgment. This work is partially supported by the National Project for the Development of Key Fundamental Sciences in China, by the National Natural Science Foundation of China, by the Foundation of Ministry of Education of China, and by the Foundation of the Chinese Academy of Science. Hai Lin thanks FB9-Chemie, Universität Wuppertal, and the Alexander von Humboldt Research Fellowship for finishing the final stage of this work.

References and Notes

(1) Quack, M. *Annu. Rev. Phys. Chem.* **1990**, *41*, 839.
(2) Fermi, E. *Z. Phys.* **1931**, *71*, 250.
(3) Marquardt, R. R.; Quack, M.; Stohner, J.; Sutcliffe, E. *J. Chem. Soc., Faraday Trans. 2* **1986**, *82*, 1173.
(4) Dübal, H.-R.; Quack, M. *J. Chem. Phys.* **1984**, *81*, 3779.
(5) Segall, J.; Zare, R. N.; Dübal, H.-R.; Lewerenz, M.; Quack, M. *J. Chem. Phys.* **1987**, *86*, 634.
(6) Pine, A. S.; Fraser, G. T.; Pliva, J. M. *J. Chem. Phys.* **1988**, *89*, 2720.
(7) Pine, A. S.; Pliva, J. M. *J. Mol. Spectrosc.* **1988**, *130*, 431.
(8) Wong, J. S.; Green, W. H.; Cheng, C.; Moore, C. B. *J. Chem. Phys.* **1987**, *86*, 5994.
(9) Lewerenz, M.; Quack, M. *Chem. Phys. Lett.* **1986**, *123*, 197.
(10) Hollenstein, H. A.; Lewerenz, M.; Quack, M. *Chem. Phys. Lett.* **1990**, *165*, 175.
(11) Manzanares, C.; Yamasaki, N. L. S.; Weitz, E. *Chem. Phys. Lett.* **1988**, *144*, 43.
(12) Ross, A. J.; Hollenstein, H. A.; Marquardt, R. R.; Quack, M. *Chem. Phys. Lett.* **1989**, *156*, 455.
(13) Davidsson, J.; Gutow, J. H.; Zare, R. N.; Hollenstein, H. A.; Marquardt, R. R.; Quack, M. *J. Phys. Chem.* **1991**, *95*, 1201.
(14) Marquardt, R. R.; Goncalves, N. S.; Sala, O. *J. Chem. Phys.* **1995**, *103*, 8391.
(15) Amrein, A.; Dübal, H.-R.; Lewerenz, M.; Quack, M. *Chem. Phys. Lett.* **1984**, *112*, 387.
(16) Segall, J.; Zare, R. N.; Dübal, H.-R.; Lewerenz, M.; Quack, M. *J. Chem. Phys.* **1987**, *86*, 634.
(17) Dübal, H.-R.; Ha, T.-K.; Lewerenz, M.; Quack, M. *J. Chem. Phys.* **1989**, *91*, 6698.
(18) Kauppi, E.; Halonen, L. *J. Chem. Phys.* **1989**, *90*, 6980.
(19) Halonen, L.; Kauppi, E. *J. Chem. Phys.* **1990**, *92*, 3278.
(20) Kauppi, E. *J. Mol. Spectrosc.* **1994**, *167*, 314.
(21) Mecke, R. *Z. Electrochem.* **1950**, *54*, 38.
(22) Lin, H.; Yuan, L. F.; He, S. G.; Wang, X. G. Zhu, Q. S. *J. Chem. Phys.* **2000**, *112*, 7484.
(23) Ha, T.-K.; Lewerenz, M.; Marquardt, R. R.; Quack, M. *J. Chem. Phys.* **1990**, *93*, 7097.
(24) Luckhaus, D.; Quack, M. *Chem. Phys. Lett.* **1993**, *205*, 277.
(25) Lin, H.; Yuan, L. F.; He, S. G.; Wang, X. G. *J. Chem. Phys.* **2001**, *114*, 8905.
(26) Lin, H.; Yuan, L. F.; He, S. G.; Wang, X. G. *Chem. Phys. Lett.* **2000**, *332*, 569.
(27) Halonen, L.; Carrington, T., Jr.; Quack, M. *J. Chem. Soc., Faraday Trans. 2* **1988**, *84*, 1371.
(28) Becke, A. D. *J. Chem. Phys.* **1993**, *98*, 5648. Perdew, J. P.; Wang, Y. *Phys. Rev. B* **1992**, *45*, 13244.
(29) Hay, P. J.; Wadt, W. R. *J. Chem. Phys.* **1985**, *82*, 270.
(30) Raghavachari, K.; Trucks, G. W. *J. Chem. Phys.* **1989**, *91*, 1062 and references therein.
(31) Herzberg, G. *Molecular Spectra and Molecular Structure*; Van Nostrand Reinhold: New York, 1945; Vol. II, Chapter 3.
(32) Papoušek, D.; Aliev, M. R. *Molecular Vibrational-Rotational Spectra*; Elsevier Scientific Publishing Company: Amsterdam, 1982.
(33) Lewerenz, M.; Quack, M. *J. Chem. Phys.* **1988**, *88*, 5408.
(34) Kjaergaard, H. G.; Henry, B. R. *J. Chem. Phys.* **1992**, *96*, 4841.
(35) Fair, J. R.; Votava, O.; Nesbitt, D. J. *J. Chem. Phys.* **1998**, *108*, 72.
(36) Lin, H.; Bürger, H.; Mkadmi, E. B.; He, S. G.; Yuan, L. F.; Breidung, J.; Thiel, W.; Huet, T. R.; Demaison, J. *J. Chem. Phys.* **2001**, *115*, 1378.
(37) Le Sueur, C. R.; Miller, S.; Tennyson, J.; Sutcliffe, B. T. *Mol. Phys.* **1992**, *76*, 1147.
(38) Eckart, C. *Phys. Rev.* **1935**, *47*, 552. Pulay, P.; Fogarasi, G.; Pang, F.; Boggs, J. E. *J. Am. Chem. Soc.* **1979**, *101*, 2550.
(39) Bunker, P. R. *Molecular Symmetry and Spectroscopy*; Academic Press: New York, 1979; Chapter 7.
(40) He, S. G.; Zheng, J. J.; Hu, S. M.; Lin, H.; Ding, Y.; Wang, X. H.; Zhu, Q. S. *J. Chem. Phys.* **2001**, *114*, 7018.
(41) Lin, H.; Yuan, L. F.; Wang, D.; Zhu, Q. S. *Chin. Phys. Lett.* **2000**, *17*, 13.
(42) Lin, H.; Bürger, H.; He, S. G.; Yuan, L. F.; Breidung, J.; Thiel, W. *J. Phys. Chem. A* **2001**, *105*, 6065.
(43) Hampel, C.; Peterson, K.; Werner, H.-J. *Chem. Phys. Lett.* **1992**, *190*, 1 and references therein.
(44) Green, W. H.; Lawrance, W. D.; Moore, C. B. *J. Chem. Phys.* **1987**, *86*, 6000.